Proceedings of ERAD 2006

Water vapor and liquid water estimates using simultaneous S and Ka band radar measurements

Scott Ellis[1], Jothiram Vivekanandan[1]

[1] National Center for Atmospheric Research, Boulder CO (USA).

1 Introduction

Using simultaneous S and Ka band observations it is possible to retrieve a path integrated value of the water vapor content as well as cloud liquid water content values using the atmospheric and liquid water attenuation properties at the two frequencies. Recently the NCAR S-band dual polarimetric (S-Pol) radar has been upgraded to include simultaneous Ka-band radar measurements (Farquharson et al, 2005). The Ka band antenna is mounted on the side of the S-band antenna and the two radars have matched beam widths and range resolutions.

Atmospheric, or gaseous, attenuation at radio frequencies is mainly due to absorption by water vapor molecules with a small contribution by molecular oxygen. The attenuation depends on the concentrations of the absorbing gases, temperature and pressure. At Ka-band, the attenuation due to oxygen small, predictable and can be accounted for because molecular is oxygen evenly distributed in the troposphere. The temperature dependence, which is weak, and pressure dependence are accurately accounted for by layer based radiative transfer models (Liebe 1985). Thus, in principle, it is possible to estimate a path integrated value of water vapor content from accurate atmospheric attenuation estimates.

The liquid water attenuation through clouds can also be estimated by comparing simultaneous S and Ka-band reflectivity values. Vivekanandan et al (1999) showed that cloud liquid water content (LWC) is linearly related to Ka-band attenuation. This is an extremely useful result because the attenuation based retrieval of LWC is independent of the unknown drop size distribution (DSD). Variations of DSD's constitute a major source of error in radar retrievals of hydrometeor mass. Combining LWC with reflectivity Vivekanandan et al (1999) showed that it is possible to estimate the median volume diameter (MVD).

The data used in the current study were obtained from the Rain In Cumulus over the Ocean (RICO) experiment conducted in December and January 2004/2005 in the Caribbean Sea. This data set is ideal because there were numerous trade wind cumulus clouds for LWC retrievals and providing different radar paths for the humidity retrieval. For comparison of the dual-wavelength LWC and humidity retrievals, aircraft measurements of LWC, dropsondes and upsondes were available.

2 Water Vapor Retrieval Method

The proposed method for retrieval of water vapor from dual wavelength radar observations includes three steps: 1. Selection of appropriate data, 2. Estimation of Ka-band atmospheric attenuation, and 3. Retrieval of humidity using a radiative transfer model.

2.1 Data selection

There are a number of criteria that have been developed to ensure the data used in the water vapor retrieval are appropriate. A small patch of data is selected, currently by hand, at the edges of weather echoes nearest the radar in order to avoid contamination by liquid water attenuation. Liquid attenuation at Ka-band is much stronger than gaseous absorption (by approximately a factor of 60). Therefore patches of data selected did not extend more than 0.5 km into any weather echo.

The power returned from Bragg scatter can be strong at S-band, and is generally much smaller at Ka-band. Data must be selected that is not significantly affected by the Bragg scatter power associated with the turbulence at the edges of clouds. The edges of the liquid cloud echo can be roughly determined by the Ka-band reflectivity. The selected data must have S-band reflectivity values at least 5 dBZ above the observed Bragg scatter echoes surrounding the liquid cloud.

The selected data must satisfy the Rayleigh scattering approximation for both radar wavelengths. Drop diameters of less than roughly 1 mm satisfy this condition. Only data with average differential reflectivity (ZDR) values less than 0.25 dB and reflectivity (Z) less than 20 dBZ are allowed. Further the median dropsize diameter, D_0, is estimated from Z and ZDR (Beard and Chaung, 1987). If the mean D_0

exceeds 0.5 mm the data are rejected. A reasonable approximation of maximum drop size is $2*D_0$ (Vivekanandan, personal communication).

The effects of partial beam blockage and point targets such as birds must also be avoided. To help identify any problems a point by point correlation coefficient between S- and Ka-band reflectivity values over each data patch is computed. Data with less than 0.7 correlation are rejected.

2.2 Atmospheric attenuation estimation

The difference between S-band and Ka band reflectivity in the absence of absorption by liquid water, violation of the Rayleigh approximation and contamination by radar Bragg scatter and other radar artifacts, can be used to obtain an accurate estimate of the atmospheric attenuation along the radial.

Once suitable data have been selected the average S- and Ka-band reflectivity values and average range are computed. The averages of reflectivity are computed in linear units. The two-way gaseous attenuation (dB km-1) is estimated simply as the difference of mean S-band dBZ and mean Ka band dBZ values divided by range.

2.3 Humidity estimation

With the atmospheric attenuation estimation along a radial, it is possible to infer the path integrated water vapor content using a full radiative transfer model. The model used in this study is from Liebe (1985) and computes the attenuation due to water vapor and molecular oxygen absorption over propagation paths through atmospheric layers defined by their depth as well as pressure and temperature at the bottom and top of the layers.

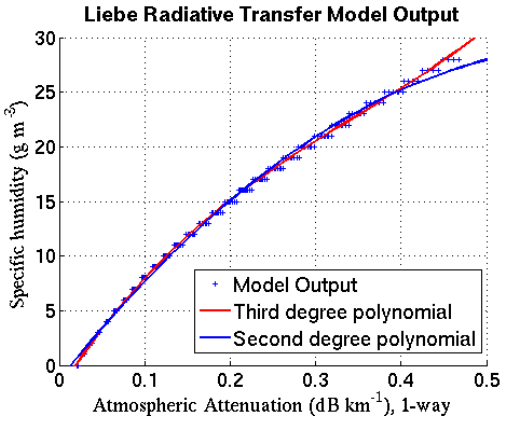

Fig 1. Scatter plot of specific humidity (g m-3) versus one-way attenuation (dB km-1), overlaid with second (blue solid line) and third (red solid line) polynomial fit curves.

The model was run numerous times over the range of temperatures and pressures found in RICO over the boundary layer. Figure 1 shows a scatter plot of the model computed specific humidity (g m^{-3}) versus one-way atmospheric attenuation (dB km^{-1}). The tight scatter indicates that the temperature and pressure dependence over the range of values in question are small. Both second and third degree polynomial fits were computed and are plotted in Figure 1. The third degree polynomial fit was chosen for the retrieval algorithm and yielded the following equation for specific humidity (SH, in g m^{-3}),

$$SH = 201.40A_a^3 - 209.60A_a^2 + 120.55A_a - 2.25, \quad (1)$$

where A_a is the one-way atmospheric attenuation (dB km^{-1}).

It is also possible to make atmospheric attenuation estimates of segments of rays not beginning at the radar if the attenuation from the radar to the beginning of the ray segment can be accounted for. This is the case for multiple clouds at different ranges. These ray segments are referred to as secondary rays, while estimates from the radar to a cloud are called primary rays.

3 LWC and MVD retrieval method

The liquid water content retrieval has similar data requirements as the humidity estimation. Thus the criteria described in section 2.1 were applied to cloud echoes. A Rayleigh scattering mask was then constructed denoting regions of Rayleigh scattering at both Ka and S-bands. Next the Ka-band attenuation by cloud liquid could be estimated and finally the liquid water content and median volume diameter were estimated.

3.1 Cloud liquid attenuation estimation

The proposed attenuation estimate is a modified version of the method of Tuttle and Rinehart (1983), which was designed for the S and X-band observations of the NCAR CP-2 radar. At X-band it is mainly hailstones that are large enough to violate the Rayleigh scattering approximation. Thus, Tuttle and Rinehart (1983) could make the reasonable assumption that Rayleigh conditions were met at the edges of cloud echoes due to the unlikely appearance of hail there. This assumption is not valid for Ka-band observations, because drops $\geq$ 1 mm occur regularly at the edge of convective cells. After the S and Ka-band reflectivity values are smoothed using a two dimensional triangular filter, the total Ka attenuation along a ray segment within a cell is estimated using regions determined to be Rayleigh scattering. These regions need not be at the nearest and farthest edge of the echo relative to the radar. Following Tuttle and Rinehart (1983), the attenuation and reflectivity data are then fit to solve for the coefficient C in the equation for attenuation,

$$A_c = CZ_s^p, \quad (2)$$

where A_c is the one-way Ka-band cloud attenuation (dB km^{-1}), Z_s is the S-band reflectivity in mm^6 m^{-3} and p is a constant. The length of a ray segment within the cell is required to be > 2 km to make a valid attenuation estimate. Once the coefficient C is determined for a ray segment, the range resolved Ka-band attenuation is determined using Equation (2). This allows attenuation estimates through the entire cloud, including regions violating the Rayleigh scattering approximation. There are cases in which no suitable attenuation estimate can be computed due to a lack

of Rayleigh scatterers within the cloud, or if a negative attenuation value is computed. Negative values of estimated attenuation can occur due to a weak signal combined with measurement errors, or a failure in the determination of regions with Rayleigh scattering. In these rays, an average value of C computed for the rest of the cloud is used to retrieve the attenuation.

3.2 LWC and MVD estimation

With the range-resolved cloud attenuation estimates (A_c, dB km^{-1}) obtained as described in section 3.1, the liquid water content (g m^3) was estimated using the relationship developed by Vivekanandan et al. (1999), i.e.,

$$LWC = 0.74A_c. \quad (3)$$

This relationship is valid for a temperature of –10 ^oC, which is far colder than the roughly 25 ^oC clouds observed during RICO. Cloud attenuation is a function of temperature and equation (3) needed to be adjusted to account for the warmer environment. Thus the radiation model of Liebe (1985) was used to compute a correction factor to account for the temperature difference.

Next the median volume diameter was computed from the LWC estimates and S-band reflectivity values following the relationship, (Vivekanandan et al., 1999),

$$MVD^3 = 2.16 \times 10^{-4}\ Z/LWC \quad (4)$$

where MVD is in mm, Z is in mm6 m-3 and LWC is g m^{-3}.

4 Results

The path integrated humidity, as well as range resolved LWC and MVD estimates were computed with data from the Rain in Cumulus over the Ocean (RICO) data. Sounding data and aircraft data were available for comparison. The NCAR C-130 was penetrating the trade wind cumulus clouds with two King LWC probes and also releasing dropsondes.

4.1 Humidity results

The dual-wavelength radar retrievals of path integrated humidity can be plotted with height using the elevation of the mid-point of the ray segment used, resulting in a vertical profile that can be compared to upsonde or dropsonde data. Figure 2 shows humidity (g m^{-3}) retrievals (plus and dot symbols) from the 10th and 12th of January compared to proximity sounding data (solid line). The plus symbols denote primary rays and the dots secondary rays (as described in section 2.3). It can be seen from Figure 2 that the retrievals agree well with the sounding data. Both the magnitude of humidity and the vertical trend agree well.

The root mean square difference between the retrievals and the soundings were computed to be 0.85 and 0.75 g m-3 on the 10th and 12th of January, respectively. For the given pressure and temperature conditions, one g m^{-3} is roughly equivalent to one degree C dewpoint temperature.

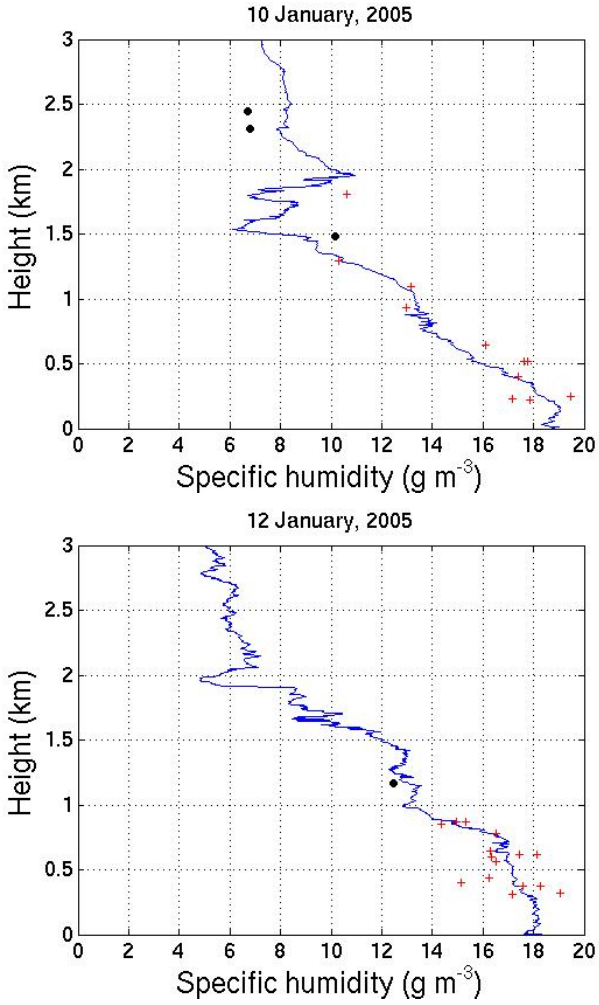

Fig 2. Plots of dual-wavelength radar retrieved LWC (g m^{-3}) from RICO (plus symbols represent primary rays and dots secondary rays) and proximity sounding data (solid line) for 10 January (top panel) and 12 January (bottom panel).

4.2 LWC and MVD results

The liquid water content retrieval for a PPI scan on 12 January that was in a region the C-130 aircraft was flying through the clouds making LWC measurements. The C-130 aircraft is actually visible in the reflectivity field as it exited a small cumulus cell (Figure 3). This is confirmed by the aircraft track, plotted as a white line in Figure 3. Therefore for this case the time and space matching of the aircraft and radar data are excellent. The LWC retrieval is shown in Figure 4. A thorough comparison of dual-wavelength radar retrieved LWC to aircraft measurements has not yet been completed. Nevertheless, the King probe was measuring between 0.1 and 0.5 g m^{-3} of cloud water through the southernmost portion of the cell labelled A in Figure 3. This is in close agreement with the LWC retrieved from the dual-wavelength radar data in that region.

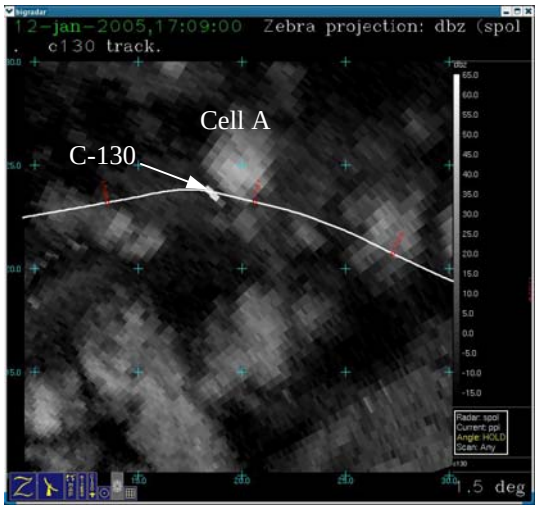

Fig 3. PPI plot of S-band reflectivity (dBZ) on 12 January, 2005. The flight track of the C-130 is plotted as the solid white line. The reflectivity signature of the C-130 aircraft can clearly be seen as it exited the southernmost portion of a trade wind cumulus cloud labelled cell A.

A PPI plot of the retrieved median volume diameter is shown in Figure 5. To date, there is no comparison to in-situ measurements of MVD, however the majority of values are reasonable. There are a few rays containing significantly larger values than neighboring rays. This is likely caused by underestimates of cloud attenuation along these rays resulting in underestimates of LWC. From equation (4) it is seen that MVD is inversely proportional to LWC, so an underestimate in LWC results in an overestimate of MVD.

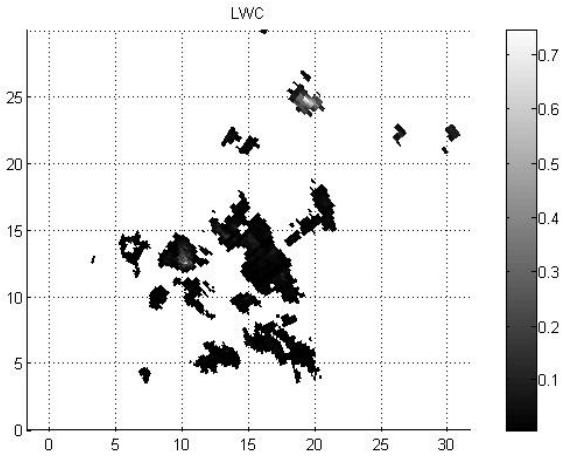

Fig 4. PPI plot of dual-wavelength radar retrieved LWC (g m^{-3})

While judgement on the performance of the LWC and MVD retrievals must be reserved for a more rigorous comparison with in-situ measurements, it is encouraging that the initial results are reasonable.

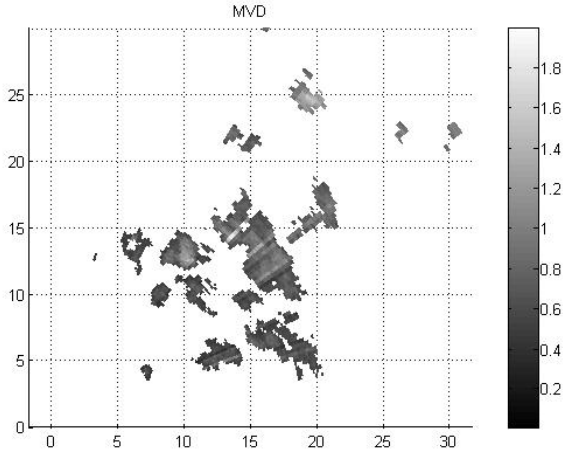

Fig 5. PPI plot of dual-wavelength radar retrieved MVD (mm)

Acknowledgements: Portions of this work were sponsored by the National Science Foundation. The views expressed in the paper are those of the authors and do not necessarily represent the official policy position of the U.S. government. The authors would like to thank Paul Field for helpful discussions concerning the aircraft data and to Chris Burghart for helping with the ZEBRA software to.

References

Beard, K. V., and C. Chuang, 1987: A new model for the equilibrium shape of reaindrops. J. Atmos. Sci., **44**, 1509-1524

Farquharson, G., F. Pratte, M. Pipersky, D. Ferraro, A. Phinney, E. Loew, R. A. Rillng, S. M. Ellis, and J. Vivekanandan, 2005: NCAR S-Pol Second Frequency (Ka-band) Radar. 32nd Conf. on Radar Meteor. AMS, Albuquerque, N.M.

Liebe, H. J., 1985: An updated model for millimeter wave propagation in moist air. *Radio Sci*., **20**, 1069 – 1089

Tuttle, J. D., and R. E. Rinehart, 1983: Attenuation correction in dual-wavelength analyses, *J. Clim. Appl. Meteor*., **22**, no. 11, 1914-1921.

Vivekanandan, J., B. Martner, M.K. Politovich and G. Zhang, 1999: Retrieval of atmospheric liquid and ice characteristics using dual-wavelength radar observations. *IEEE Trans. On Geoscience and Remote Sensing*, **37**, 2325-2334.